Deuterium Exchange in the Systems of H_2O^+/H_2O and H_3O^+/H_2O

Vincent G. Anicich and Atish D. Sen[1]

Jet Propulsion Laboratory,
California Institute of 'J'ethnology,
4800 Oak Grow Drive,
Pasadena, CA 91109,
MS 183/601

Current Address - Department of Atmospheric Sciences, University of California, Los Angeles, CA 90095

Abstract

Using tandem mass spectrometry the H_2O^+, H_3O^+, D_2O^+, and D_3O^+ ions were observed to interact with the H_2O and D_2O neutrals. The reactions consisted of a series of charge transfer, proton transfer, and isotopic exchange steps. The experimental data sets consist of variations of ion abundance's over the neutral pressure range from O to $2x1$ O-s Torr. An expected sequence of isotopic exchange reactions is specified. An exact solution of the set of differential equations was determined for the reactions of ionized water and then for protonated water. A linear regression technique was then used to determine the individual reaction rate coefficients from the experimental data.

Branching ratios and relative reactions rate coefficients were determined. The statistical analysis showed that only an evaluation of the primary isotopic exchange processes is significant, The errors in the determinations of subsequent channels increased rapidly. The analysis introduced in this work was applied to SIFT data published previously. Statistical analysis of the results shows that determination of a specific mechanism is not justified.

2

Introduction

Part of the water system which is reported here was previously studied b y selected ion flow tube (SIFT) technology While. conclusions of the original study were not disproven, it was re-analyzed. Additional data from the tandem (ICR) provides new information on the SIFT technology and the conclusions previously reported from that work.

Only a few ion-molecule systems have been studied for deuterium scrambling. This is an important process that needs to be quantified. Deuterium is prevalen in our solar system and is present in interstellar space. The ratios of hydrogen and deuterium in various molecule.s and the isotopic fractionation processes occuring in these regions are of great relevance to interpreting the cosmic abundances. The fundamental ion-molecule reaction that needs to b e measured is the reaction between an ion and neutral which have only one deuterium atom between them: i.e. it can be present in either the ion or the neutral.

Partially deuterated systems are particularly difficult to study, principally due to the cost of the materials and the quantities needed to passivate the experiment. Deuterium exchange reactions are also very difficult to study because of the rapid rates of exchange, the number of consecutive steps, and the extent of the branching that occurs. In the case of water, where the experimental apparatus retains the isotopic species for a long time because of the adhesion of the water to the various surfaces of the experiment, the purity of the neutral isomer cannot be validated. Even when a tandem experiment is used and the ion mass is preselected, the rate of isotopic scrambling makes the certainty of a specific mass' isomeric composition questionable. A case in point is the ion HDO^+ which has a mass of 19 Dalton, but which cannot be distinguished from the H_3O^+ ion.

The conclusion of Smith *et al.*[1] was that the deuterium exchange in the H_3O^+/D_2O and D_3O^+/H_2O systems behaved as a purely statistical process. They conclude also that the reactions proceed through a long-lived association complex which lives sufficiently long enough to randomize the H's and D's before unimolecular decomposition can occur. These results were for the thermal neutral isotopic exchange reactions between H_3O^+ and D_2O and between D_3O^+ and H_2O.

They also published in the same paper-1 the reaction of D_3O^+ and NH_3 a n d found very different results. In this proton transfer reaction only D^+ w a s transferred. In this case they concluded that a long lived intermediate complex was not formed. Similar results were found with CD_5^+/NH_3 and other asymmetric exothermic proton transfer reactions

These types of studies are reported in published work in 1976[2,3]. Through ICR studies[3], charge transfer reactions in the near- thermoneutral symmetric systems, $^{15}N_2^+/^{14}N_2$, $^{14}N_2^+/^{15}N_2$, $^{12}CO^+/^{13}CO$, and $^{13}CO^+/^{12}CO$ were found to have reactions rate coefficients which are half of the collision rate. This suggested a statistical mechanism. The rates of hydrogen exchange in the reactions of H_2D^+/HD, HD_2^+/HD, and $^{14}NH_4^+/^{15}NH_3$ were all found to have reactions rate coefficients which would be expected from a statistical model[3]. The two systems $CH_3D_2^+/CH_2D_2$ and $CH_2D_3^+/CH_2D_2$ could not be explained by such a mechanism

Subsequent work has been published o n H_3O^+/D_2O, D_3O^+/H_2O, NH_4^+/ND_3, ND_4^+/NH_3, CH_5^+/CD_4, and CD_5^+/CH_4[4]. In this work the reactions were analyzed b y considering the average number of proton/deuteron jumps, κ, occurring during the lifetime of the intermediate. The water system was determined to be long lived compared to the shuttling time and therefore gave statistical exchanges, $\kappa \geq$ 20. Ammonia and methane systems were found to have increasingly shorter lived complexes compared to the shuttling time and therefore gave less and less opportunity for statistical results, κ = 025 for methane.

4

Experimental

The experiments were performed on a tandem mass spectrometer with the configuration ICR-Dempster-ICR[5,6]. The instrument is built within a 12 inch electromagnet. This supplied the magnetic field for all three sections of the instrument. The source was a two section ICR drift cell. A 180° magnetic sector was used as the primary mass filter. Typically a 3 kilovolt electric field was used as the acceleration field and the magnetic field was adjusted to give ions with the appropriate velocity to enter the deceleration- energy selection region in front of the second ICR. After the ions were decelerated, a long narrow Wien filter was used to limit the ion energies to less than 30 meV before they enter the second ICR. The second ICR was also a two section drift cell. The second section was used to measure the reaction of the ions from the entrance through the detection region. A Wronka bridge detector[7] was used to monitor the ion abundances. Frequency scans on the detector were used to obtain a mass spectrum in the second ICR.

Gases used were from distilled water and deuterated water. Both samples were purified by several freeze-pump-thaw cycles. To insure a predominance of H_2O^+ and D_2O^+ from the source, the pressure in the source was limited so that very little protonated water was evident. The source output was mass analyzed using only the Dempster sector and an auxiliary current detector. To insure a predominance of H_3O^+ and D_3O^+ from the source, the pressure in the source was increased until the protonated water was dominant species. Many minutes were required before the pressure and the isotopic purity became stable in both the source and the analyzer.

The pressure in the second ICR was measured directly using a Baratron capacitance manometer which had a 1 Torr head. At lower pressures an ion gauge was used and calibrated against the Baratron at higher pressures.
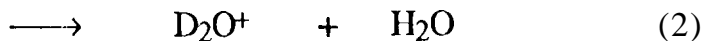
The drift time was not measured directly. The rate constants of the known water reactions were used as a reference and other rate constants were measured relative to these.
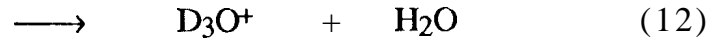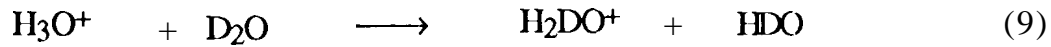
Results and Discussion

Four sets of data were taken. They consist of values of the fractional abundance[s] of the ion concentrations versus the bath pressure. The data sets for the reactant pairs: H_3O^+/D_2O, D_3O^+/H_2O, D_2O^+/H_2O, and H_2O^+/D_2O are shown i n Figures 1 through 4. In general, the starting ion is lost rapidly, then several isomeric species are formed and in the end a single ion dominates. Several consecutive reactions are possible at the highest pressures. The terminal ion is H_3O^+ when H_2O is the neutral and D_3O^+ when D_2O is the neutral. The intermediate steps in the reaction pathway are assumed to be a combination of charge transfer, proton transfer, and isotopic exchange reactions.
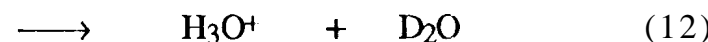
Data Analyses

The analyses of the data consisted of a least squares regression. The model used is listed below. The first set of reactions is for a bath of D_2O.

$$H_2O^+ + D_2O \longrightarrow HDO^+ + HDO \tag{1}$$
$$\longrightarrow D_2O^+ + H_2O \tag{2}$$
$$\longrightarrow H_2DO^+ + OD \tag{3}$$
$$\longrightarrow HD_2O^+ + OH \tag{4}$$

$$HDO^+ + D_2O \longrightarrow D_2O^+ + HDO \tag{5}$$
$$\longrightarrow HD_2O^+ + CD \tag{6}$$
$$\longrightarrow D_3O^+ + OH \tag{7}$$

$$D_2O^+ + D_2O \longrightarrow D_3O^+ + OD \tag{8}$$

6

$$H_3O^+ \;+\; D_2O \;\longrightarrow\; H_2DO^+ \;+\; HDO \qquad (9)$$
$$\longrightarrow\; HD_2O^+ \;+\; H_2O \qquad (1o)$$

$$H_2DO^+ \;+\; D_2O \;\longrightarrow\; HD_2O^+ \;+\; HDO \qquad (11)$$
$$\longrightarrow\; D_3O^+ \;+\; H_2O \qquad (12)$$

$$HD_2O^+ \;+\; D_2O \;\longrightarrow\; D_3O^+ \;+\; HDO \qquad (13)$$

This second set of reactions is for a bath of H_2O.

$$D_2O^+ \;+\; H_2O \;\longrightarrow\; HDO^+ \;+\; HDO \qquad (1)$$
$$\longrightarrow\; H_2O^+ \;+\; D_2O \qquad (2)$$
$$\longrightarrow\; HD_2O^+ \;+\; OH \qquad (3)$$
$$\longrightarrow\; H_2DO^+ \;+\; OD \qquad (4)$$

$$HDO^+ \;+\; H_2O \;\longrightarrow\; H_2O^+ \;+\; HDO \qquad (5)$$
$$\longrightarrow\; H_2DO^+ \;+\; OH \qquad (6)$$
$$\longrightarrow\; H_3O^+ \;+\; OD \qquad (7)$$

$$H_2O^+ \;+\; H_2O \;\longrightarrow\; H_3O^+ \;+\; OH \qquad (8)$$

$$D_3O^+ \;+\; H_2O \;\longrightarrow\; HD_2O^+ \;+\; HDO \qquad (9)$$
$$\longrightarrow\; H_2DO^+ \;+\; D_2O \qquad (10)$$

$$HD_2O^+ \;+\; H_2O \;\longrightarrow\; H_2DO^+ \;+\; HDO \qquad (11)$$
$$\longrightarrow\; H_3O^+ \;+\; D_2O \qquad (12)$$

$$H_2DO^+ \;+\; H_2O \;\longrightarrow\; H_3O^+ \;+\; HDO \qquad \mathbf{(13)}$$
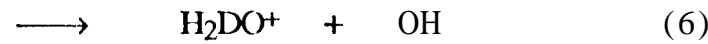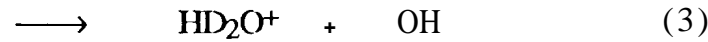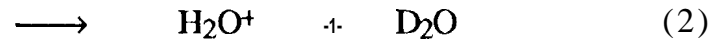
The reactions numbers are duplicated under the assumption that the symmetry of the reactions makes them identical. The solutions to the two sets of simultaneous differential equations are shown in the Appendices 1 and 2 for each of the two experiment types: the first having ionized water as the starting ion and the second having protonated water as the starting ion. These solutions were then used in a least squares regression to fit to the experimental data.

These solutions are shown in Figures 1 through 4 as solid lines. The numerical values are lists in Tables 1 and 2.

A fifth data set was taken from the work of Smith, Adams, and Henchman. This fifth set consists of values of the fractional abundance[s] of the ion concentrations versus the bath pressure for the reactant pair D_3O^+/H_2O. The data and fit of this data set is shown in Figure 5.

With the regression technique it was possible to determine the one sigma[9], or 68% confidence level of the branching ratios. This was accomplished b y varying the branching ratio until the square of the sum of errors was quadrupled. The present ICR data had a sigma of 0.014 for the H_3O^+/H_2O branching ratios and 0.021 for the H_2O^+/H_2O branching ratios. The single SIFT data set had a sigma of 0.021 for the H_3O^+/H_2O branching ratios, showing that the SIFT data was a little noisier.

Conclusions

Both the ICR results and the SIFT results agree within the 68% confidence level for the H_3O^+/H_2O data. The statistical ratios expected from the model of Smith, Adams, and Henchman, two to one, are within the error limits of each experiment, but the error limits are, $\pm$ 0.10 for the ICR experiment and $\pm$ 0.23 for the SIFT experiment. There is too large an uncertainty in the results to define the statistical model as a unique explanation, but certainly cannot not b e excluded.

All the channels were determined with some statistical certainty except the reactions of the singly labeled ion, HDO^+. 'l'he analysis method used in this work was unable to evaluate the rates of Reactions 5 through 7. All channels were shown to have a finite probability, but the statistical errors were larger then the determined values.

The possible products of the reaction of H_2O^+ with D_2O included: charge transfer, with and without isotopic scrambling and self protonation of H_2O^+, with and without isotopic scrambling. All possible products of the proton /deuteron exchange reactions of H_3O^+ were observed.

If it assumed that the literature value for the self protonation reaction of H_2O^+ and H_2O, k_8, is also the proton transfer rate. for reactions 1 through 4 and 5 through 7, and that the total of the charge transfer and proton transfer reaction rates are equal to the collision rate, then the measured rates, k_{1-4} and k_{5-7}, should be equal to the collision rate minus the rate of the systematic charge transfer reaction. If the symmetric charge transfer channels are assumed to b e statistically accessed, then $k_{(1-4)} = 2.78 \times 10^{-9} cm$ 3/s and $k_{(5-8)} = 2.41$ xl $0^9 cm^3/s$. . These are both consistent with the experimental results.

The measured ratios of the change transfer channels 1 and 2 are not consistent with a statistical distribution of protons and deuterons. We therefore conclude while the proton transfer reactions are apparently statistical because they go through a collision complex, the charge transfer reactions are n on-statistical and do not go through a collision complex.

If, for the proton scrambling reactions, the reactions proceed at the collision rate less the statistical symmetric reaction fraction, then $k_{(9-10)} =$ 2.60x 10-9 cm^3/s, $k_{(11-12)} = 2.02x$ 10-9 cm^3/s, and $k_{(13)} = 1$ .16x10-9 cm^3/s. These are all consistent with the experimental results.

Acknowledgments

References

1. D. Smith, N.G. Adams, and M.J. Henchman, *J. Chem. Phys. 72, 4951 (1980).*

2. A. G. Harrison, P. -H. Lin, and C. W. Tsang, *Int. J. Mass Spectrom. Ion Phys.* **19,** 23 (1976).

3. T.B. McMahon, P.G. Miasek, and J.L.. Beauchamp, *Int. J. Mass Spectrom. Ion Phys., 21, 63 (1976).*

4. N.G. Adams, D. Smith, and M.J. Henchman, *Int. J. Mass Spectrom. Ion Phys., 42,* 11 (1982); M. Henchman, D. Smith, N.G. Adams, J.F. Paulson, and Z. Herman, *Int. J. Mass Spectrom. Ion Proc., 92, 15 (1989);* M.J. Henchman, D. Smith, and N.G. Adams, *Int. J. Mass Spectrom. Ion Phys., 109, 105 (1 991).*

5. V. G. Anicich, A.D. Sen, W.T. Huntress, Jr., and M.J. McEwan, *J. Chem. Phys.,* **102, 3256 (1995).**

6. P.R. Kemper and M.T. Bowers, *Int. J. Mass Spectrom. Ion Phys., 52, 1(1 983).*

7. J. Wronka and D.P. Ridge, Rev. *Sci. Instrum., 43, 49* (1982).

8. V. G. Anicich, *J. Phys. Chem. Ref. Data, 22, 1469 (1 993).*

9. W.H. Press, S.A. Teukolsky, W.T. Vetterling, and B.P. Flannery, "Numerical Recipes in FORTRAN, The Art of Scientific Computing," 2nd Ed. (Cambribge Press, New York, 1992).

Table 1. Summary of Analysis of the H_3O^+/H_2O Systems

	D_3O^+/H_2O, SIFT		H_3O^+/D_2O, SIFT	D_3O^+/H_2O		H_3O^+/D_2O		Sat
b_9	0.68	±.23	0.70	0.49	±.10	0.42	±.10	0.67
b_{10}	0.32	±.23	0.30	0.51	±.10	0.58	±.10	0.33
$k_{9\text{-}10}$	2.20	±36%	2.27	2.20	±15%	2.20	±15%	
b_{11}	0.64	±.27	-	1.00	>.62	1.00	>.66	0.86
b_{12}	0.36	±.27	-	0.00	<.38	0.00	<.34	0.14
$k_{11\text{-}12}$	1.56	±55%	-	3.22	±60%	2.32	±70%	
k_{13}	0.75	±35%	-	0.80	±100%	0.62	±50%	

k's in unit of $(\times 10^{-9})\ cm^3 s^{-1}$.

Table 2. Summary of Analysis of the H_2O^+/H_2O Systems

	D_2O^+/H_2O		H_2O^+/D_2O		Sat
b_1	0.08	±.22	0.22	±.20	0.26
b_2	0.14	±.16	0.41	±.15	0.0-?
b_3	0.34	±.16	0.00	±.15	0.33
b_4	0.44	±.16	0.37	±.15	0.33
$k_{1\text{-}4}$	4.00	±50%	3.62	±50%	
b_5	-		-		0,23
b_6	-		-		0,19
b_7	-		-		0.58
$k_{5\text{-}7}$	-		-		
k_8			-		

k's in unit of $(\times 10^{-9})\ cm^3 s^-$
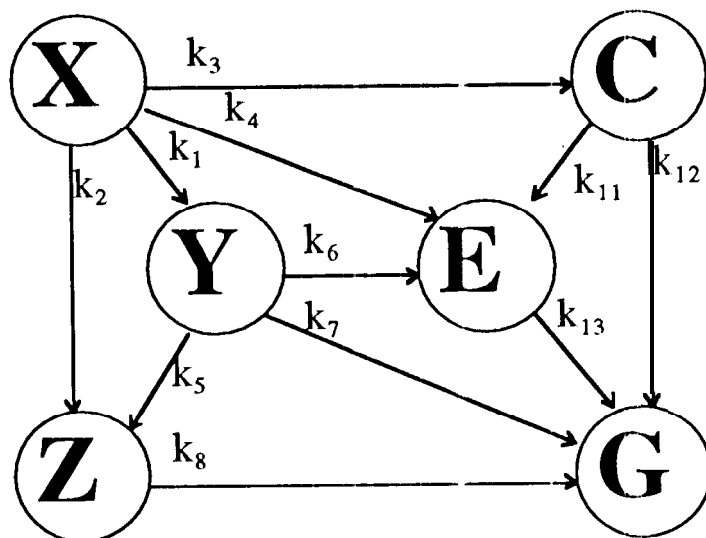
The Solution

$$[A] = [A]_0 \exp[-(k_9 + k_{10})[B]t$$

$$[C] = [A]_0 \frac{k_9}{[k_9 + k_{10} - (k_{11} + k_{12})]} \left[\exp[-(k_{11} + k_{12})[B]t] - \exp[-(k_9 + k_{10})[B]t] \right]$$

$$[E] = \left| \begin{array}{l} [A]_0 \left[\dfrac{k_{10}}{k_9 + k_{10} - k_{13}} \right] \left[\exp[-k_{13}[B]t] - \exp[-(k_9 + k_{10})[B]t] \right] \\[2em] +[A]_0 \left[\dfrac{kg}{k_9 + k_{10} - (k_{11} + k_{12})} \right] \left\| \begin{array}{l} \dfrac{k_{11}}{[k_{11} + k_{12}] - k_{13}} \left[\exp[-k_{13}[B]t] - \exp[-(k_{11} + kn)[B]t] \right] \\[2em] - \dfrac{k_{11}}{[k_9 + k_{10} - k_{13}} \left[\exp[-k_{13}[B]t] - \exp[-(k_9 + k_{10})[B]t] \right] \end{array} \right\| \end{array} \right|$$

$$[G = 1 - [A] - [C] - [E]$$

Appendix 2

The Problem

$$\frac{d[X]}{dt} = -(k_1 + k_2 + k_3 + k_4)[X][B]$$

$$\frac{d[Y]}{dt} = k_1[X][B] - (k_5 + k_6 + k_7)[Y][B]$$

$$\frac{d[Z]}{dt} = k_2[X][B] + k_5[Y][B] - k_8[Z][B]$$

$$\frac{d[C]}{dt} = k_3[X][B] - (k_{11} + k_{12})[C][B]$$

$$\frac{d[E]}{dt} = k_4[X][B] + k_6[Y][B] + k_{11}[C][B] - k_{13}[E][B]$$

$$\frac{d[G]}{dt} = k_7[Y][B] + k_8[Z][B] + k_{12}[C][B] + k_{13}[E][B]$$

The Solution

$$[X] = [X]_0 \exp[-(k_1 + k_2 + k_3 + k_4)[B]t$$

$$[Y] = [X]_0 \left[\frac{k_1}{k_1 + k_2 + k_3 + k_4 - (k_5 + k_6 + k_7)} \right] \left[\exp[-(k_5 + k_6 + k_7)[B]t] \cdot \exp[-(k_1 + k_2 + k_3 + k_4)[B]t] \right]$$

$$[Z] = \left| \begin{array}{l} [X]_0 \dfrac{k_2}{\left[k_1 + k_2 + k_3 + k_4 - k_8\right]} \left[\exp[-k_8[B]t] - \exp[-(k_1 + k_2 + k_3 + k_4)[B]t] \right] \\[3mm] + [X]_0 \dfrac{k_1}{\left[k_1 + k_2 + k_3 + k_4 - (k_5 + k_6 + k_7)\right]} \left[\begin{array}{l} \dfrac{k_5}{\left[k_5 + k_6 + k_7 - k_8\right]} \left[\exp[-k_8[B]t] - \exp[-(k_5 + k_6 + k_7)[B]t] \right] \\[3mm] - \dfrac{k_5}{\left[k_1 + k_2 + k_3 + k_4 - k_8\right]} \exp[-k_8[B]t] - \exp[-(k_1 + k_2 + k_3 + k_4)[B]t] \end{array} \right] \end{array} \right|$$

$$[C] = [X]_0 \frac{k_3}{\left[k_1 + k_2 + k_3 + k_4 - (k_{11} + k_{12})\right]} \left[\exp[-(k_{11} + k_{12})[B]t] - \exp[-(k_1 + k_2 + k_3 + k_4)[B]t] \right]$$

$$[E] = \left| \begin{array}{l} [X]_0 \dfrac{k_4}{\left[k_1 + k_2 + k_3 + k_4 - k_{13}\right)} \left[\exp[-k_{13}[B]t] - \exp[-(k_1 + k_2 + k_3 + k_4)[B]t] \right] \\[3mm] + [X]_0 \dfrac{k_1}{\left[k_1 + k_2 + k_3 + k_4 - (k_5 + k_6 + k_7)\right]} \left[\begin{array}{l} \dfrac{k_6}{\left[k_5 + k_6 + k_7 - k_{13}\right]} \left[\exp[-k_{13}[B]t] - \exp[-(k_5 + k_6 + k_7)[B]t] \right] \\[3mm] - \dfrac{k_6}{\left[k_1 + k_2 + k_3 + k_4 - k_{13}\right]} \left[\exp[-k_{13}[B]t] - \exp[-(k_1 + k_2 + k_3 + k_4)[B]t] \right] \end{array} \right] \\[5mm] + [X]_0 \left[\dfrac{k_3}{k_1 + k_2 + k_3 + k_4 - (k_{11} + k_{12})} \right] \left[\begin{array}{l} \left[\dfrac{k_{11}}{k_{11} + k_{12} - k_{13}} \right] \left[\exp[-k_{13}[B]t] - \exp[-(k_{11} + k_{12})[B]t] \right] \\[3mm] - \dfrac{k_{11}}{\left[k_1 + k_2 + k_3 + k_4 - k_{13}\right]} \left[\exp[-k_{13}[B]t] - \exp[-(k_1 + k_2 + k_3 + k_4)[B]t] \right] \end{array} \right] \end{array} \right|$$

$$[G] = 1 - [X] - [Y] - [Z] - [C] - [E]$$

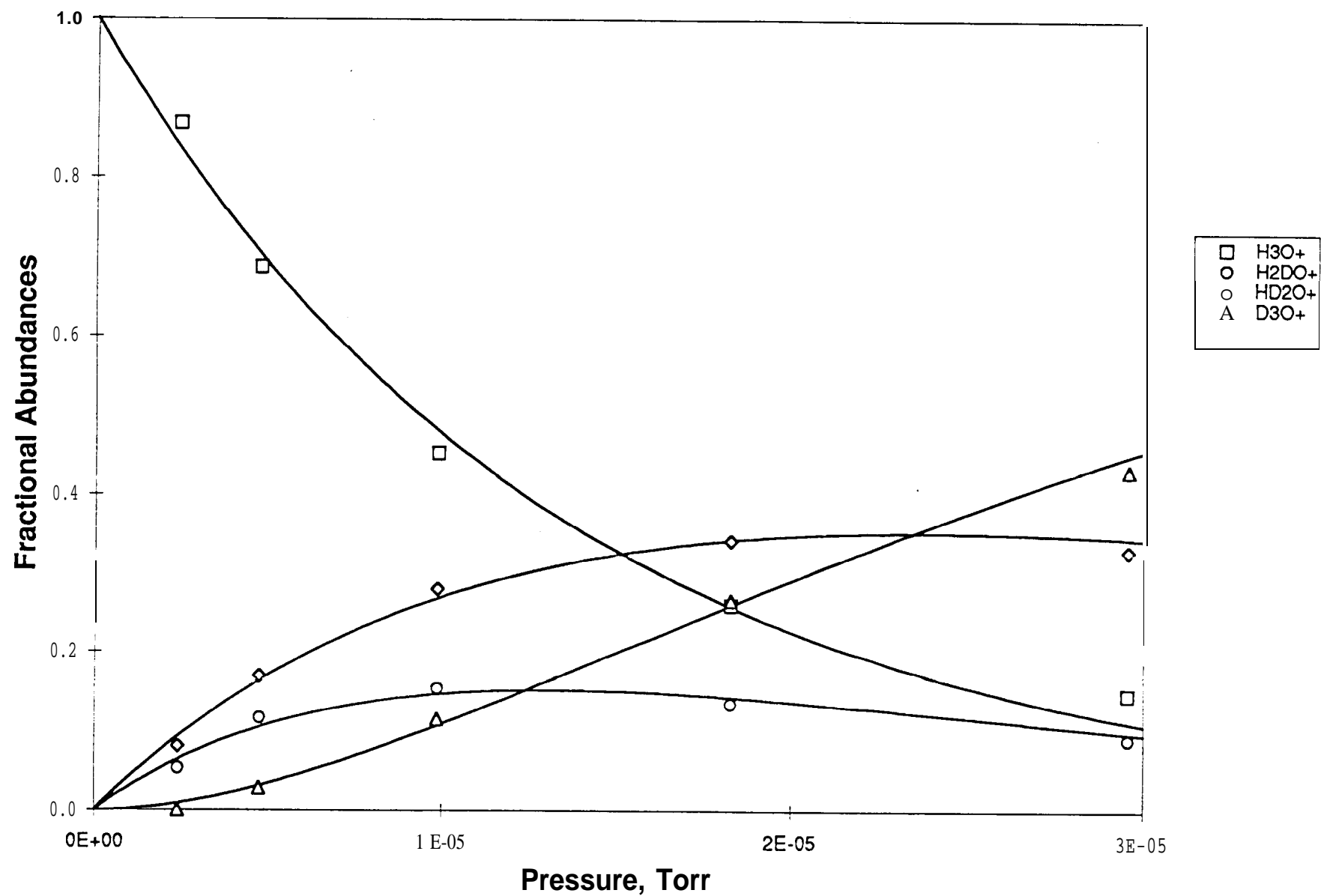Figure 1. Ion abundances in the isotropic exchanges reactions starting with H3O+ in a D20 bath. From the tandem ICR-Dempster-ICR spectrometer. The points represent the data and the line a modeled fit.
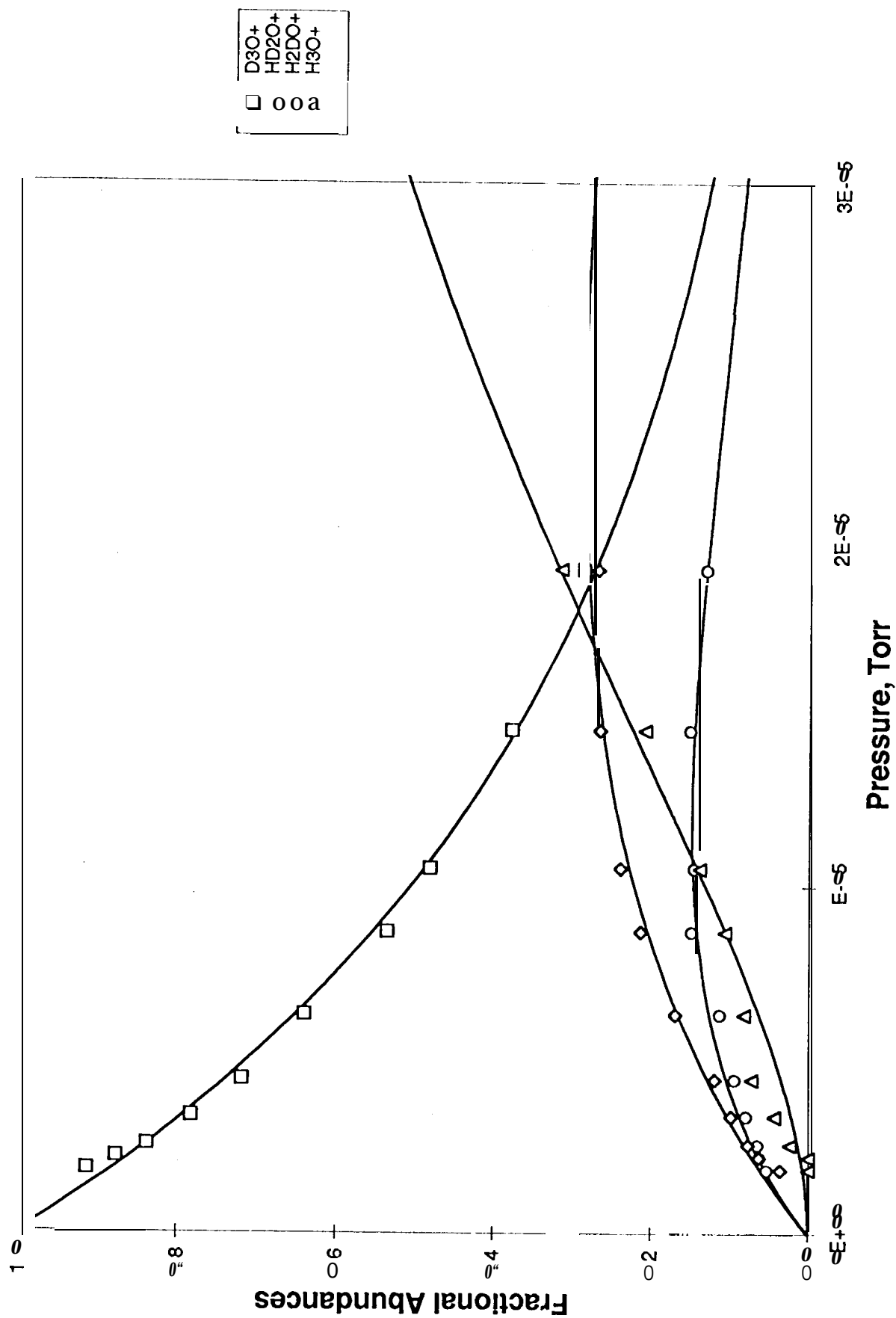
Figure 2. Ion abundances in the isoptopic exchange reactions starting with D3O+ in an H2O bath. From the tandem ICR-Dempster-ICR spectrometer. The points are the data and the line a modeled fit.
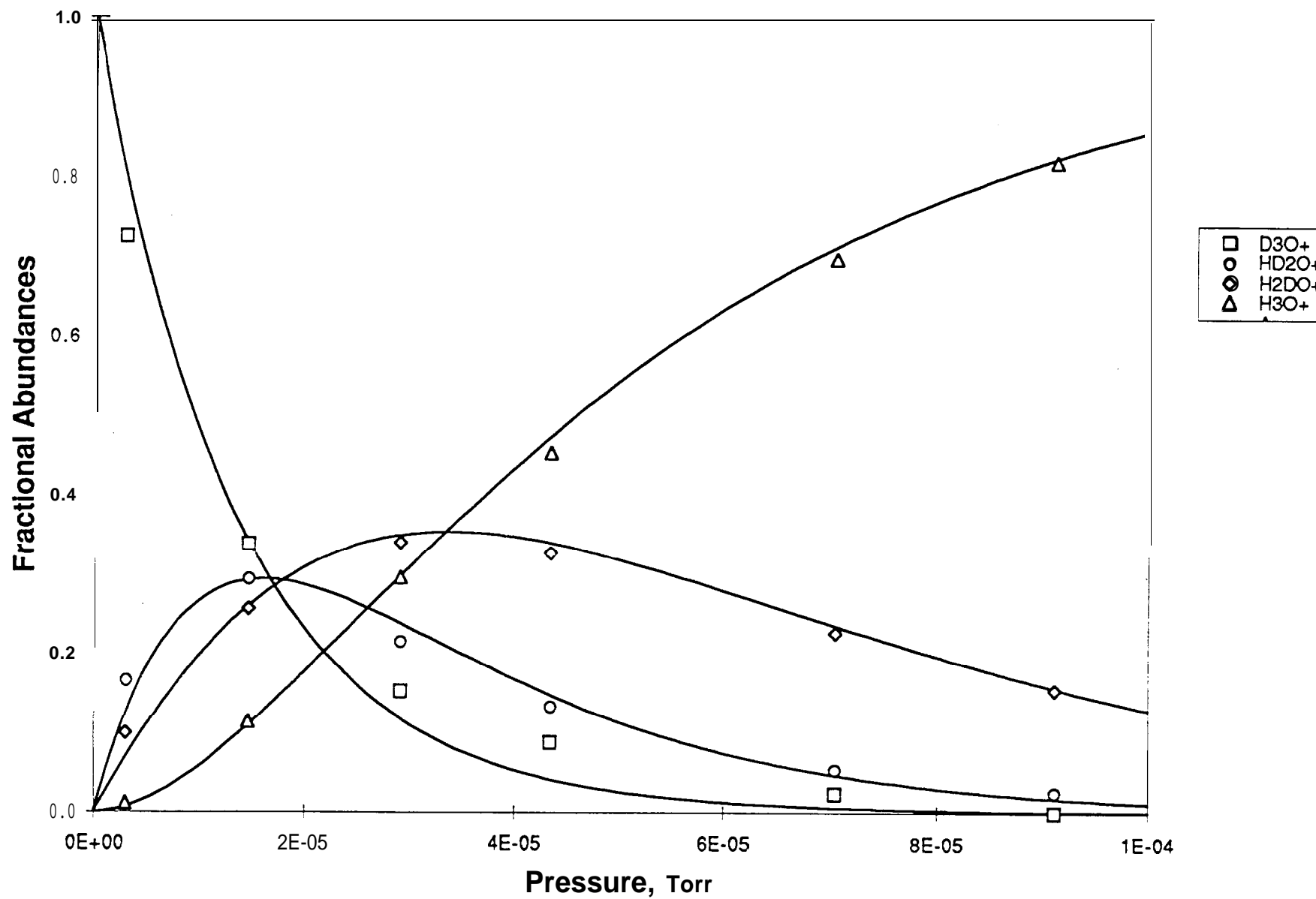
Figure 3. Ion abundances in the isotopic exchange reactions starting with D3O+ in a H20 bath. From Reference 1 a SIFT experiment. The points are the data and the line a modeled fit.

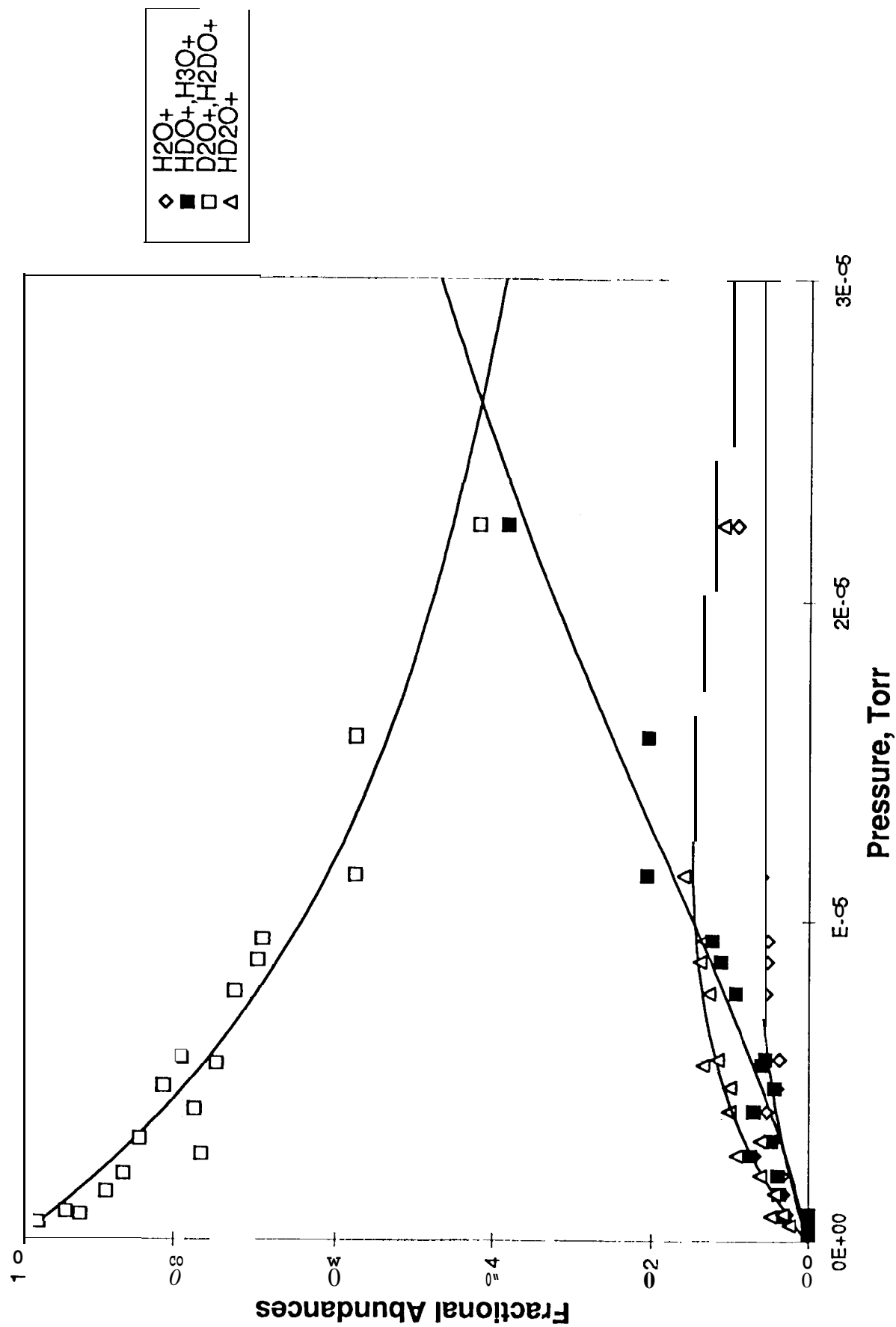Figure 4. Ion abundances in the isotopic exchange reactions starting with D2O+ in a H2O bath. From the tandem ICR-Dempster-ICR spectrometer. The points represent the data and the lines a modeled fit.

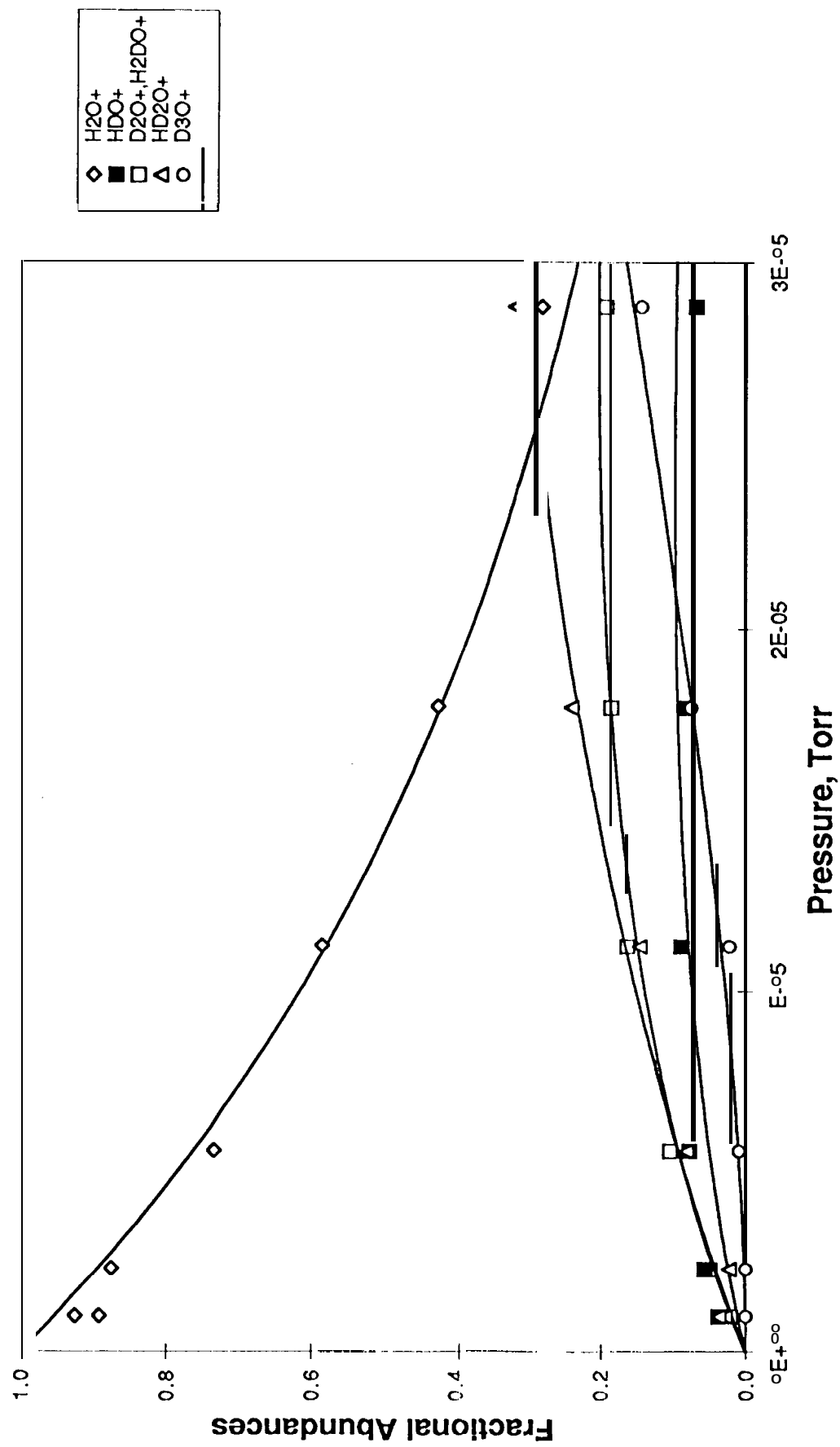Figure 5. Ion abundances in the isotopic exchange reactions starting with H2O+ in a D2O bath. From the tandem ICR-Dempster-ICR spectrometer. The points represent the data and the lines a modeled fit.